

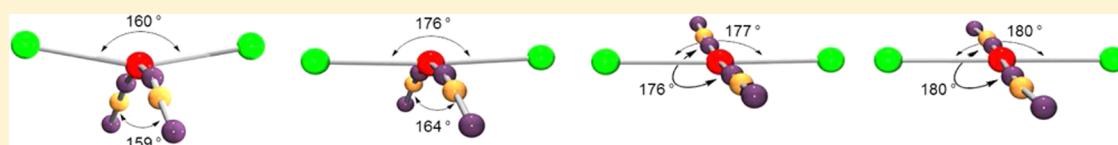
Pendant Alkyl and Aryl Groups on Tin Control Complex Geometry and Reactivity with H₂/D₂ in Pt(SnR₃)₂(CNBu^t)₂ (R = Bu^t, Prⁱ, Ph, Mesityl)

Anjaneyulu Koppaka,[†] Lei Zhu,[†] Veeranna Yempally,[†] Derek Isrow,[†] Perry J. Pellechia,[‡] and Burjor Captain^{*,†}

[†]Department of Chemistry, University of Miami, Coral Gables, Florida 33124, United States

[‡]Department of Chemistry and Biochemistry, University of South Carolina, Columbia, South Carolina 29208, United States

Supporting Information



ABSTRACT: The complex Pt(SnBu^t)₂(CNBu^t)₂(H)₂, **1**, was obtained from the reaction of Pt(COD)₂ and Bu^t₃SnH, followed by addition of CNBu^t. The two hydride ligands in **1** can be eliminated, both in solution and in the solid state, to yield Pt(SnBu^t)₂(CNBu^t)₂, **2**. Addition of hydrogen to **2** at room temperature in solution and in the solid state regenerates **1**. Complex **2** catalyzes H₂–D₂ exchange in solution to give HD. The proposed mechanism of exchange involves reductive elimination of Bu^t₃SnH from **1** to afford vacant sites on the Pt center, thus facilitating the exchange process. This is supported by isolation and characterization of Pt(SnMes₃)(SnBu^t)(CNBu^t)₂, **3**, when the addition of H₂ to **2** was carried out in the presence of free ligand Mes₃SnH (Mes = 2,4,6-Me₃C₆H₂). Complex Pt(SnMes₃)₂(CNBu^t)₂, **5**, can be prepared from the reaction of Pt(COD)₂ with Mes₃SnH and CNBu^t. The exchange reaction of **2** with Ph₃SnH gave Pt(SnPh₃)₃(CNBu^t)₂(H), **6**, wherein both SnBu^t₃ ligands are replaced by SnPh₃. Complex **6** decomposes in air to form square planar Pt(SnPh₃)₂(CNBu^t)₂, **7**. The complex Pt(SnPrⁱ)₂(CNBu^t)₂, **8**, was also prepared. Out of the four analogous complexes Pt(SnR₃)₂(CNBu^t)₂ (R = Bu^t, Mes, Ph, or Prⁱ), only the Bu^t analogue does both H₂ activation and H₂–D₂ exchange. This is due to steric effects imparted by the bulky Bu^t groups that distort the geometry of the complex considerably from planarity. The reaction of Pt(COD)₂ with Bu^t₃SnH and CO gas afforded *trans*-Pt(SnBu^t)₂(CO)₂, **9**. Compound **9** can be converted to **2** by replacement of the CO ligands with CNBu^t via the intermediate Pt(SnBu^t)₂(CNBu^t)₂(CO), **10**.

INTRODUCTION

The chemistry of compounds containing a transition metal–tin bond has a long history,^{1–3} sparked in part by the fact that certain heterogeneous catalysts were found to be more active in the presence of tin as a promoter.^{4–13} Recent developments, particularly with respect to ligand design, have led to a renaissance in this area, and a number of metal–tin complexes with unique structures have been discovered.^{10,14–27} Tin compounds have been used extensively as modifiers of the platinum group metals, and platinum–tin bimetallic heterogeneous catalysts have been shown to be highly efficient for use in the petroleum industry for a number of processes vital to petroleum reforming,^{28–33} catalytic hydrogenations,^{34–37} and dehydrogenations.^{38,39} In the area of homogeneous catalysis, tin complexes have been utilized for hydrogenation and isomerization of olefins,^{7,40–42} the water–gas shift reaction,^{43,44} and also improvement of the product selectivities of the reactions.^{3,8,45} The trimetallic-tin containing catalyst PtRu₅Sn was recently shown to exhibit the highest selectivity for formation of unsaturated alcohols in the hydrogenation of citral.⁹

Of the several methods available to prepare transition metal–tin complexes, oxidative addition of triaryl- and trialkylstannanes (R₃SnH) is one of the most general and versatile pathways. Reductive elimination of R₃SnH can also occur readily, and the “balance point” with respect to the oxidative addition/reductive elimination of stannanes is a function of both the substituents on the given metal complex and the nature of the alkyl or aryl substituents on tin. In spite of considerable work in the area of transition metal–tin chemistry, the factors controlling the reactivity of these complexes are largely empirical in nature.

The sterically encumbered stannane, tri-*tert*-butyltin hydride, Bu^t₃SnH, has great potential; however, there is not much chemistry associated with this compound in the literature. To demonstrate the versatility of this new ligand, we have already prepared a few metal complexes from reactions of Bu^t₃SnH with metal carbonyl compounds. Reaction of Bu^t₃SnH with Pt₂Ru₄(CO)₁₈ yields the new trimetallic Pt/Ru/Sn mixed metal cluster Pt₂Ru₂(CO)₉.

Received: November 3, 2014

Published: December 24, 2014

(SnBu_3)₂(μ -H)₂, which was shown to be a hydrogenation catalyst when supported on mesoporous silica.⁴⁶ The coordination chemistry of bulky tin ligands with cobalt and nickel⁴⁷ and with iron^{10,48} has also been investigated. Recently it was shown that reversible activation of hydrogen by the bimetallic Pt–Sn complex Pt(SnBu_3)₂(CNBu^t)₂, **2**, occurs rapidly not only in solution but also in the solid state.²²

The current work reports synthetic, structural, and reaction chemistry on a series of bimetallic Pt–Sn complexes in which the stannanes studied have different steric and electronic properties and include tri-*tert*-butyl stannane (Bu_3SnH), trimesitylstannane (Mes_3SnH , $\text{Mes} = 2,4,6\text{-Me}_3\text{C}_6\text{H}_2$), triphenylstannane (Ph_3SnH), and triisopropylstannane (Pr_3SnH). Important points are the interaction of these complexes with dihydrogen and their ability to do H₂–D₂ exchange, as well as other reactions relevant to these. Oxidative addition of R₃SnH, while generally favorable in the Pt(0) to Pt(II), is shown to be more readily reversible in the Pt(II) to Pt(IV) manifold. A complex picture emerges in which the nature of the R group on the coordinated stannane alters both the structure and the reactivity of the Pt complex.

EXPERIMENTAL SECTION

General Data. Unless indicated otherwise, all reactions were performed under an atmosphere of argon. Reagent-grade solvents were dried by the standard procedures and were freshly distilled prior to use. Infrared spectra were recorded on a Nicolet 380 FT-IR spectrophotometer. ¹H NMR were recorded on a Bruker 300 and 400 spectrometer operating at 300.13 and 399.99 MHz, respectively. Elemental analyses were performed by Columbia Analytical Services (Tucson, AZ). Mass spectrometric measurements, performed by a direct exposure probe using electron impact ionization (EI), were made on a VG 70S instrument at the University of South Carolina, Columbia, SC, and ESI-TOF measurements were performed using micrOTOF-Q II at University of Miami. *tert*-Butyl isocyanide, CNBu^t , was purchased from Sigma-Aldrich and used without further purification. Triphenyltin hydride was purchased from Alfa Aesar and used without further purification. Bis(1,5-cyclooctadiene)platinum, Pt(COD)₂,⁴⁹ Bu_3SnH ,^{10,48} Mes_3SnH ,⁵⁰ and Pr_3SnH ⁵¹ were prepared according to the published procedures. Product separations were performed by TLC in air on Analtech silica gel GF 250 or 500 μm glass plates.

Synthesis of Pt(SnBu_3)₂(CNBu^t)₂(H)₂, **1.** In a glovebox, under an atmosphere of argon, 49.5 mg of Bu_3SnH (0.170 mmol) dissolved in 5 mL of freshly distilled hexane was added to 35.0 mg of Pt(COD)₂ (0.085 mmol). The reaction mixture was stirred at room temperature for 5 min, after which time 14.0 mg of CNBu^t (0.170 mmol) was added, and the reaction mixture stirred at room temperature for an additional 10 min. The solution was then filtered, and the filtrate was placed in a –20 °C freezer overnight, which gave crystalline Pt(SnBu_3)₂(CNBu^t)₂(H)₂, **1**. After the crystalline product was washed with approximately 2 mL of acetonitrile, 26.0 mg (32% yield) of **1** was obtained. Spectral data for **1**: ¹H NMR (C_6D_6 , rt, in ppm) $\delta = 1.57$ (s, 54 H, SnBu_3 , ³J_{Sn–H} = 51 Hz), 0.96 (s, 18 H, Bu^t), –13.52 (s, 2 H, hydride, ¹J_{Pt–H} = 697 Hz, ²J_{Sn–H} = 34 Hz); ¹¹⁹Sn{¹H} NMR (C_6D_6 , rt, in ppm) $\delta = 81.50$ (s, 2 Sn, ¹J_{Pt–Sn} = 3604 Hz); IR (cm^{-1} in hexane) $\nu_{\text{CN}} = 2139$ (s), $\nu_{\text{Pt–H}} = 2112$ (m); EI/MS $m/z = 942$ (M^+), 883 ($\text{M}^+ - \text{H}_2 - \text{Bu}^t$). The isotope pattern is consistent with the presence of one platinum and two tin atoms.

Conversion of Pt(SnBu_3)₂(CNBu^t)₂(H)₂, **1, to Pt(SnBu_3)₂(CNBu^t)₂, **2**, in Solution.** A 15.0 mg amount of **1** (0.016 mmol) was dissolved in 50 mL of distilled hexane. With stirring, argon was then purged through the solution at 25 °C for approximately 20 h. Within minutes, the colorless solution started to turn violet. ¹H NMR of the reaction mixture showed complete conversion of the starting **1** to **2**. The solvent was removed *in vacuo*, and the violet residue was crystallized by evaporation of a benzene/acetonitrile

solvent mixture under a stream of argon at room temperature to yield 13.2 mg (88%) of **2**. Spectral data for **2**: ¹H NMR (C_6D_6 , rt, in ppm) $\delta = 1.60$ (s, 54 H, SnBu_3 , ³J_{Sn–H} = 49 Hz), 1.15 (s, 18 H, Bu^t); IR (cm^{-1} in hexane) $\nu_{\text{CN}} = 2112$ (s); EI/MS $m/z = 940$ (M^+), 883 ($\text{M}^+ - \text{Bu}^t$). The isotope pattern is consistent with the presence of one platinum and two tin atoms.

Conversion of Pt(SnBu_3)₂(CNBu^t)₂, **2, to Pt(SnBu_3)₂(CNBu^t)₂(H)₂, **1**, in Solution.** In a 10 mL Schlenk tube, 28.0 mg of **2** (0.030 mmol) was dissolved in 5 mL of hexane. The solvent was removed under a slow stream of hydrogen gas (approximately 3 h), during which time the color of the solution changed from violet to colorless. This yielded 26.2 mg (93% yield) of crystalline **1**.

Conversion of Pt(SnBu_3)₂(CNBu^t)₂(H)₂, **1, to Pt(SnBu_3)₂(CNBu^t)₂, **2**, in the Solid State.** In a 10 mL Schlenk tube containing 10.0 mg of colorless crystalline **1** (0.011 mmol), argon gas was purged through the system for 24 h in the dark at room temperature, after which time the color of the crystalline **1** turned to violet. ¹H NMR indicated complete consumption of starting **1** in quantitative yield to give **2**.

Conversion of Pt(SnBu_3)₂(CNBu^t)₂, **2, to Pt(SnBu_3)₂(CNBu^t)₂(H)₂, **1**, in the Solid State.** In a 10 mL Schlenk tube containing 12.0 mg of violet crystalline **2** (0.013 mmol), hydrogen gas was purged through the system for 15 min in the dark at room temperature, after which time the color of the crystalline **2** turned to colorless. ¹H NMR indicated complete consumption of starting **2** in quantitative yield to give **1**.

Synthesis of Pt(SnMes_3)(SnBu_3)(CNBu^t)₂, **3.** In a 50 mL Schlenk flask, 80.0 mg of Pt(SnBu_3)₂(CNBu^t)₂, **2** (0.085 mmol) was dissolved in 20 mL of distilled hexane. Then, 40.6 mg of Mes_3SnH (0.085 mmol) dissolved in 10 mL of distilled hexane solvent was added dropwise over a period of 10 min while the reaction mixture was stirred. The reaction mixture was then stirred for another 1 h at room temperature under a slow stream of H₂ gas purged through the solution to give an orange colored solution. The reaction flask was kept under an atmosphere of H₂ gas and stirred for an additional 12 h at room temperature. The solvent was then removed *in vacuo* to give an orange colored residue. The residue was washed three times with 2 mL portions of cold pentane and then redissolved in a mixture of CH_2Cl_2 /hexane solvent, filtered, and crystallized at –30 °C in a glovebox to obtain 53.0 mg (55% yield) of Pt(SnMes_3)(SnBu_3)(CNBu^t)₂, **3**. Spectral data for **3**: ¹H NMR (C_6D_6 , rt, in ppm) $\delta = 0.80$ (s, 18 H, 2 CNBu^t), 1.61 (s, 27 H, Bu_3Sn), 2.16 (s, 9 H, 3-*p*-CH₃, Mes_3Sn), 2.60 (s, 18 H, 6-*o*-CH₃, Mes_3Sn), 6.78 (s, 6 CH, Mes_3Sn); IR (cm^{-1} in CH_2Cl_2) $\nu_{\text{CN}} = 2138$ (vs); EI/MS $m/z = 1071$ ($\text{M}^+ - \text{Bu}^t$), 837 ($\text{M}^+ - \text{Bu}_3\text{Sn}$).

Synthesis of Pt(SnMes_3)₂(CNBu^t)₂, **5.** A 20.0 mg (0.049 mmol) amount of Pt(COD)₂ was transferred into a 50 mL Schlenk tube, which was evacuated and filled with argon several times. To this was added 10 mL of distilled hexane under argon at –78 °C. A mixture of 46.4 mg of Mes_3SnH (0.097 mmol) and 8.1 mg of CNBu^t (0.097 mmol) dissolved in 15 mL of distilled hexane solvent was added dropwise under argon while the reaction mixture was maintained at –78 °C. The reaction mixture was stirred at –78 °C for an additional 10 min and then allowed to slowly warm to room temperature, during which time the color of the solution changed to orange. The reaction mixture was stirred at room temperature for 1 h. The solvent was removed *in vacuo*, and the product was separated by TLC using hexane solvent to give a yellow band which was then crystallized in hexane solvent at –30 °C to obtain 52.0 mg (80% yield) of crystalline Pt(SnMes_3)₂(CNBu^t)₂, **5**. Spectral data for **5**: ¹H NMR (C_6D_6 , rt, in ppm) $\delta = 0.53$ (s, 18 H, 2 CNBu^t), 2.17 (s, 18 H, 6-*p*-CH₃, 2 Mes_3Sn), 2.67 (s, 36 H, 12-*o*-CH₃, 2 Mes_3Sn), 6.82 (s, 12 CH, 2 Mes_3Sn); IR (cm^{-1} in CH_2Cl_2) $\nu_{\text{CN}} = 2154$ (vs); ES⁺/MS calculated for [M^+] = 1313, found 1313. The isotope distribution is consistent with the presence of one platinum and two tin atoms.

Synthesis of Pt(SnPh_3)₃(CNBu^t)₂(H), **6.** A 20.0 mg (0.049 mmol) amount of Pt(COD)₂ was transferred into a 50 mL Schlenk tube, which was evacuated and filled with argon several times. To this was added 10 mL of distilled hexane under argon at –78 °C. While maintaining –78 °C, a mixture of 51.2 mg of Ph_3SnH (0.146

mmol) and 8.1 mg of CNBu^t (0.097 mmol) dissolved in 15 mL of distilled hexane solvent was added dropwise to the $\text{Pt}(\text{COD})_2$ solution under argon. The reaction mixture was stirred at -78°C for 10 min and then allowed to warm to room temperature, during which time a white insoluble precipitate was observed. The reaction mixture was stirred at room temperature for an additional 1 h. The solution was filtered through a glass frit in a glovebox. The white residue was washed three times with 2 mL portions of distilled hexane. The residue was dissolved in CH_2Cl_2 /hexane mixture, filtered, and crystallized at -30°C in a glovebox to obtain 60.0 mg (86% yield) of colorless crystals of $\text{Pt}(\text{SnPh}_3)_3(\text{CNBu}^t)_2(\text{H})$, **6**. Spectral data for **6** (note: compound exhibits fluxional behavior in solution): ^1H NMR (toluene- d_8 , -20°C , in ppm) $\delta = 7.8$ – 6.9 (m, Ph), 0.83 (s, CNBu^t), 0.51 (s, CNBu^t), 0.44 (s, CNBu^t), 0.44 (s, CNBu^t), -6.63 (s, hydride, $^1J_{\text{Sn-H}} = 679$ Hz, $^1J_{\text{Pt-H}} = 647$ Hz, $^1J_{\text{Pt-H}} = 775$ Hz), -11.91 (s, hydride, $^1J_{\text{Pt-H}} = 665$ Hz, $^2J_{\text{Sn-H}} = 26.68$ Hz, $^2J_{\text{Pt-H}} = 13.95$ Hz); IR (cm^{-1} in CH_2Cl_2) $\nu_{\text{CN}} = 2190(\text{vs})$. Elemental analysis, calcd: C, 54.42; H, 4.57; N, 1.98. Found: C, 53.94; H, 4.88; N, 1.82.

Conversion of $\text{Pt}(\text{SnBu}^t)_3(\text{CNBu}^t)_2$, **2, to $\text{Pt}(\text{SnPh}_3)_3(\text{CNBu}^t)_2(\text{H})$, **6**.** In a 10 mL Schlenk tube, 10.0 mg of **2** (0.011 mmol) was dissolved in 3 mL of freshly distilled hexane, to which 13.5 mg of Ph_3SnH (0.039 mmol, 3.5 equiv) dissolved in 3 mL of hexane solvent was added dropwise over a period of 10 min while the reaction mixture was stirred. During that time the violet colored solution turned colorless, and a white precipitate was observed at the bottom of the Schlenk tube. The precipitate was washed three times with 2 mL portions of distilled cold hexane, dissolved in a CH_2Cl_2 /hexane solvent mixture, filtered, and crystallized at -30°C in a glovebox to obtain 14.0 mg (90% yield) of $\text{Pt}(\text{SnPh}_3)_3(\text{CNBu}^t)_2(\text{H})$, **6**.

Synthesis of $\text{Pt}(\text{SnPh}_3)_2(\text{CNBu}^t)_2$, **7.** A 20.0 mg (0.049 mmol) amount of $\text{Pt}(\text{COD})_2$ was transferred into a 50 mL Schlenk tube, which was evacuated and filled with argon several times. To this was added 10 mL of distilled hexane under argon at -78°C . A mixture of 34.1 mg of Ph_3SnH (0.097 mmol) and 8.1 mg of CNBu^t (0.097 mmol) dissolved in 15 mL of distilled hexane solvent was added dropwise to $\text{Pt}(\text{COD})_2$ solution under argon while maintaining the reaction mixture at -78°C . The reaction mixture was stirred at -78°C for 10 min and was then allowed to warm to room temperature, during which time the solution color changed to cloudy yellow. The reaction mixture was stirred at room temperature for an additional 12 h. The solvent was removed *in vacuo*, and the residue was dissolved in CH_2Cl_2 /octane solvent mixture, filtered, and crystallized at room temperature to obtain 44.0 mg (84% yield) of yellow colored crystals of $\text{Pt}(\text{SnPh}_3)_2(\text{CNBu}^t)_2$, **7**. Spectral data for **7**: ^1H NMR (CD_2Cl_2 , rt, in ppm) $\delta = 0.883$ (s, 18 H, 2 CNBu^t), $\delta = 7.22$ – 7.7 (m, 30 H, 2 Ph_3Sn); IR (cm^{-1} in CH_2Cl_2) $\nu_{\text{CN}} = 2165$ (vs). Elemental analysis, calcd: C, 52.05; H, 4.56; N, 2.64. Found: C, 52.10; H, 4.74; N, 2.61.

Conversion of $\text{Pt}(\text{SnPh}_3)_2(\text{CNBu}^t)_2$, **7, to $\text{Pt}(\text{SnPh}_3)_3(\text{CNBu}^t)_2(\text{H})$, **6**.** In a glovebox, 20.0 mg of $\text{Pt}(\text{SnPh}_3)_2(\text{CNBu}^t)_2$, **7** (0.019 mmol), was transferred into a vial containing 3 mL of hexane, to which Ph_3SnH (7.0 mg, 0.02 mmol) dissolved in a minimum amount of hexane solvent was added dropwise with stirring. The solution became colorless over a period of 5 min, and a white precipitate of **6** was obtained at the bottom of the vial. The precipitate was washed three times with 2 mL portions of cold hexane. The residue was dissolved in a mixture of CH_2Cl_2 /hexane solvent, filtered, and crystallized at -30°C in a glovebox to obtain 18.0 mg (90% yield) of **6**.

Conversion of $\text{Pt}(\text{SnPh}_3)_3(\text{CNBu}^t)_2(\text{H})$, **6, to $\text{Pt}(\text{SnPh}_3)_2(\text{CNBu}^t)_2$, **7**.** In a 10 mL vial, 20.0 mg of **6** (0.014 mmol) was dissolved in 3 mL of CH_2Cl_2 /octane solvent mixture and left exposed to air for about 30 min with occasional stirring of the solution. After that, the resultant cloudy solution was filtered and crystallized at room temperature to obtain 9.0 mg (60% yield) of the yellow crystals of **7**.

Synthesis of $\text{Pt}(\text{SnPr}^i)_3(\text{CNBu}^t)_2$, **8.** A 50 mg (0.122 mmol) amount of $\text{Pt}(\text{COD})_2$ was transferred into a 50.0 mL Schlenk tube,

which was evacuated and filled with argon several times. To this was added 20 mL of distilled hexane under argon at -78°C , and then 20.3 mg of CNBu^t (0.244 mmol) dissolved in 5 mL of hexane was added dropwise at -78°C . The reaction mixture was stirred for 5 min, after which time 60.8 mg of Pr^i_3SnH (0.244 mmol) dissolved in 5 mL of distilled hexane solvent was added dropwise under argon while the reaction mixture was maintained at -78°C . The reaction mixture was stirred at -78°C for an additional 5 min and then allowed to slowly warm to room temperature. Solvent was removed *in vacuo* to obtain a red colored solid. Recrystallization of the product in diethyl ether solvent at -30°C in a glovebox yielded red crystalline $\text{Pt}(\text{SnPr}^i)_3(\text{CNBu}^t)_2$, **8**. The crystals were washed with 2×0.2 mL of cold hexane and the washings were further crystallized to obtain a combined yield of 70.0 mg (67%). Spectral data for **8**: ^1H NMR (C_6D_6 , rt, in ppm) $\delta = 1.16$ (s, 18 H, 2 CNBu^t), 1.66 (d, 36 H, 12 CH_3 , 6 Pr^i), $\delta = 1.89$ (m, 6 H, 6-CH, 6 Pr^i); IR (cm^{-1} in hexane) $\nu_{\text{CN}} = 2131(\text{vs})$; EI/MS $m/z = 856$ (M^+), 813 ($\text{M}^+ - \text{Pr}^i$). The isotope distribution is consistent with the presence of one Pt and two Sn atoms.

Synthesis of $\text{Pt}(\text{SnBu}^t)_3(\text{CO})_2$, **9.** A 53.0 mg (0.129 mmol) amount of $\text{Pt}(\text{COD})_2$ was transferred into a 10 mL Schlenk tube, which was evacuated and filled with argon several times. An 80.0 mg amount of Bu^t_3SnH (0.274 mmol) dissolved in 8 mL of distilled hexane solvent was added to the $\text{Pt}(\text{COD})_2$ under argon. The brown colored reaction mixture was stirred at room temperature for 5 min, after which time CO gas was bubbled through the solution for an additional 30 min. The solution was filtered through a silica plug to give a green colored solution. The solvent was removed *in vacuo* to obtain 98.0 mg (91% yield) of green solid $\text{Pt}(\text{SnBu}^t)_3(\text{CO})_2$, **9**. Spectral data for **9**: ^1H NMR (CDCl_3 , rt, in ppm): $\delta = 1.38$ (s, 54 H, SnBu^t_3 , $^3J_{\text{Sn-H}} = 59$ Hz); ^1H NMR (C_6D_6 , rt, in ppm) $\delta = 1.44$ (s, 54 H, SnBu^t_3 , $^3J_{\text{Sn-H}} = 59$ Hz); IR (cm^{-1} in hexane) $\nu_{\text{CO}} = 2007(\text{vs})$. Elemental analysis, calcd: C, 37.57; H, 6.55. Found: C, 37.77; H, 6.42.

Synthesis of $\text{Pt}(\text{SnBu}^t)_3(\text{CNBu}^t)_2(\text{CO})$, **10.** In a glovebox, under an atmosphere of argon, a 40.0 mg (0.480 mmol) amount of CNBu^t was added to 195.0 mg of **9** (0.235 mmol) dissolved in 2 mL of freshly distilled hexane at room temperature. With the addition of CNBu^t , CO gas evolves from the reaction mixture (gas bubbles can be observed), and the green colored solution slowly turns colorless, with colorless crystals coming out of the solution. The solution was placed in a -20°C freezer overnight to obtain more crystals. The solvent was then removed, and the colorless crystals were washed with 0.2 mL of hexane to afford 219.0 mg (96% yield) of **10**. The crystals turned to purple color on prolonged exposure to air, affording **2**. Spectral data for **10**: ^1H NMR (C_6D_6 , rt, in ppm) $\delta = 1.57$ (s, 54 H, SnBu^t_3 , $^3J_{\text{Sn-H}} = 51$ Hz), 0.96 (s, 18 H, Bu^t) [note: NMR spectra recorded under a CO atmosphere]; IR (cm^{-1} in hexane) $\nu_{\text{CO}} = 2144(\text{w})$, 2112(vs), 1966(s).

Conversion of $\text{Pt}(\text{SnBu}^t)_3(\text{CNBu}^t)_2(\text{CO})$, **10, to $\text{Pt}(\text{SnBu}^t)_3(\text{CNBu}^t)_2$, **2**, in Solution.** A 17.0 mg amount of **10** (0.0175 mmol) was dissolved in 10 mL of distilled hexane. With stirring, argon gas was purged through the solution at 25°C for approximately 10 min. Within minutes the colorless solution starts to turn violet. IR of the reaction mixture showed complete conversion of the starting **10** to **2**. The solvent was removed *in vacuo*, and the violet colored residue was crystallized by evaporation of a benzene/acetonitrile solvent mixture under a stream of argon gas at room temperature to yield 15.0 mg (91%) of crystalline **2**.

Conversion of $\text{Pt}(\text{SnBu}^t)_3(\text{CNBu}^t)_2$, **2, to $\text{Pt}(\text{SnBu}^t)_3(\text{CNBu}^t)_2(\text{CO})$, **10**, in Solution.** A 17.0 mg amount of **2** (0.0181 mmol) was dissolved in 25 mL of distilled hexane. With stirring, CO gas was purged through the solution at 25°C for approximately 10 min. Within minutes the violet solution starts to turn colorless. IR of the reaction mixture showed complete conversion of the starting **2** to **10**. The solvent was removed *in vacuo*, and the violet color residue was crystallized by evaporation of a benzene/acetonitrile solvent mixture under a stream of CO gas at room temperature to yield 15.0 mg (85%) of crystalline **10**.

Conversion of $\text{Pt}(\text{SnBu}^t_3)_2(\text{CNBu}^t)_2$, **2, to $\text{Pt}(\text{SnBu}^t_3)_2(\text{CNBu}^t)_2(\text{CO})$, **10**, in the Solid State.** In a 10 mL Schlenk tube containing 10.0 mg of violet crystalline **2**, CO gas was purged through the system for 1 h in the dark at room temperature, after which time the color of the crystalline **2** turned to colorless. ^1H NMR indicated complete consumption of starting **2** to give **10** in quantitative yield.

Conversion of $\text{Pt}(\text{SnBu}^t_3)_2(\text{CNBu}^t)_2(\text{CO})$, **10, to $\text{Pt}(\text{SnBu}^t_3)_2(\text{CNBu}^t)_2$, **2**, in the Solid State.** In a 10 mL Schlenk tube containing 10.0 mg of colorless crystalline **10**, argon gas was purged through the system for 16 h in the dark at room temperature, after which time the color of the crystalline **10** turned to violet. ^1H NMR indicated complete consumption of starting **10** to give **2** in quantitative yield.

RESULTS AND DISCUSSION

The reaction of $\text{Pt}(\text{COD})_2$ (COD = cyclooctadiene) and Bu^t_3SnH in the presence of *tert*-butyl isocyanide, CNBu^t , at room temperature affords the dihydrido Pt–Sn complex $\text{Pt}(\text{SnBu}^t_3)_2(\text{CNBu}^t)_2(\text{H})_2$, **1**, in 32% yield. Compound **1** was characterized by a combination of IR, ^1H NMR, mass spectrometry, and single-crystal X-ray diffraction analyses. An ORTEP drawing of the molecular structure of **1** is shown in Figure 1, as previously reported.²²

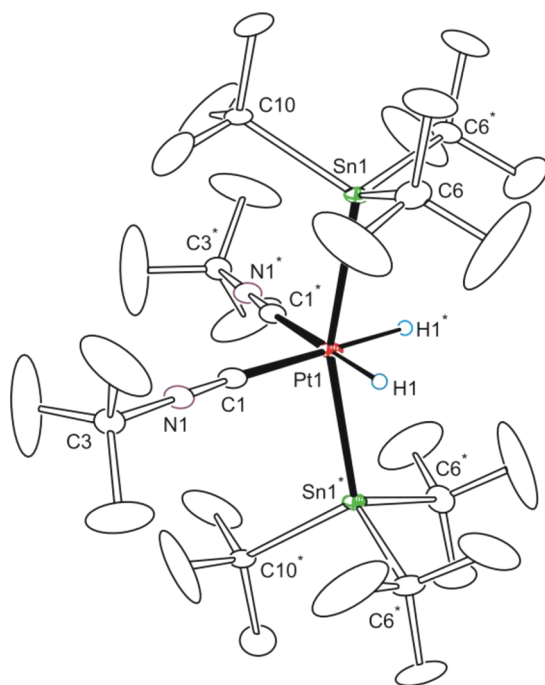


Figure 1. ORTEP⁵² drawing of the molecular structure of $\text{Pt}(\text{SnBu}^t_3)_2(\text{CNBu}^t)_2(\text{H})_2$, **1**, showing 30% probability thermal ellipsoids. Selected interatomic distances (Å) and angles (deg): Pt(1)–Sn(1) = 2.6718(5); Pt(1)–C(1) = 2.014(8); Pt(1)–H(1) = 1.65(9); Sn(1)–Pt(1)–Sn(1*) = 161.35(3); C(1)–Pt(1)–C(1*) = 102.5(4); C(1)–Pt(1)–Sn(1) = 95.82(3); Sn(1)–Pt(1)–H(1) = 84.2(4).

Compound **1** contains an 18-electron platinum atom in a distorted octahedral geometry having two SnBu^t_3 ligands, two CNBu^t ligands, and two hydride ligands such that the molecule possesses C_{2v} symmetry. The two hydrido ligands in **1** can be displaced under an atmosphere of argon gas at room temperature, both in solution and in the solid state, in nearly quantitative yields to furnish the complex $\text{Pt}(\text{SnBu}^t_3)_2(\text{CNBu}^t)_2$, **2**. Compound **2** was also characterized crystallo-

graphically, and as previously reported²² its structure in the solid state is shown in Figure 2.

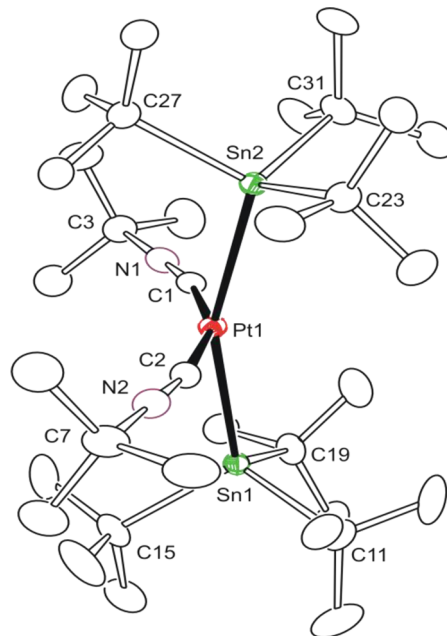
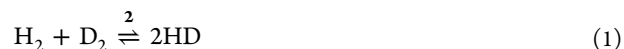


Figure 2. ORTEP⁵² drawing of the molecular structure of $\text{Pt}(\text{SnBu}^t_3)_2(\text{CNBu}^t)_2$, **2**, showing 50% probability thermal ellipsoids. Selected interatomic distances (Å) and angles (deg): Pt(1)–Sn(1) = 2.6765(3); Pt(1)–Sn(2) = 2.6851(3); Pt(1)–C(1) = 1.932(3); Pt(1)–C(2) = 1.929(3); Sn(1)–Pt(1)–Sn(2) = 159.539(8); C(1)–Pt(1)–C(2) = 158.69(13).

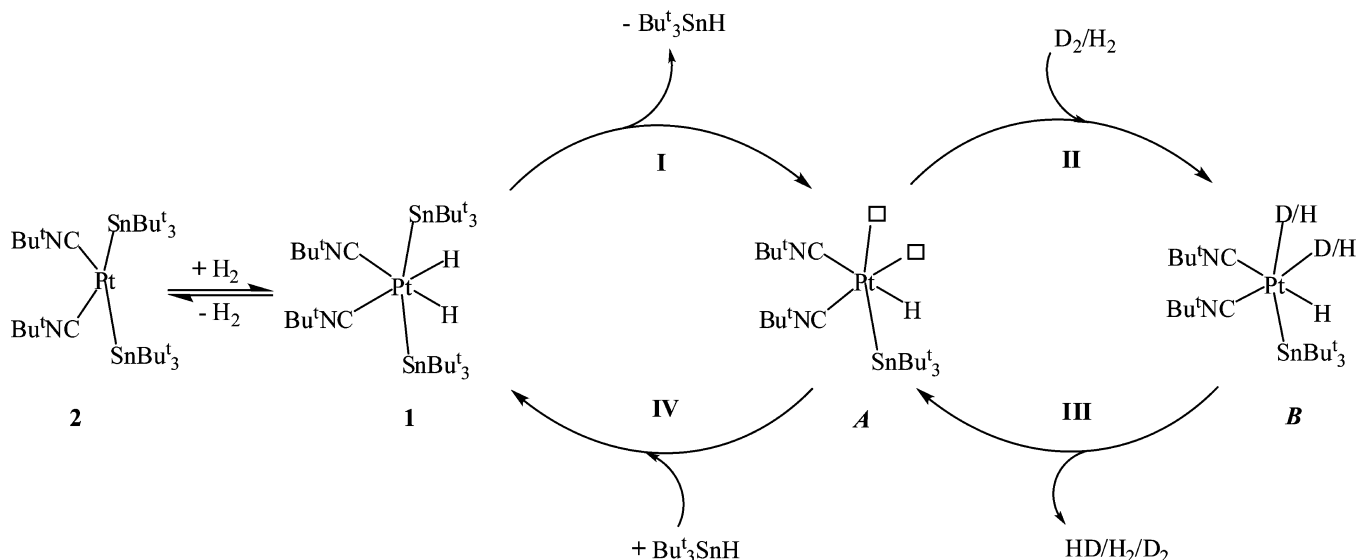
The loss of the hydride ligands gives a 16-electron configuration around the Pt atom in **2** with a formal oxidation state of +2. Complex **2** (see in Figure 2) is not planar, as expected for a Pt(II) d^8 complex; instead it adopts a “saw-horse”-type structure. This is attributed to steric pressure imparted by the bulky Bu^t groups. Addition of hydrogen gas to **2**, both in solution and in the solid state, regenerates **1**. The complex **1-d₁** was prepared by the reaction of **2** with HD gas and did not show H/D coupling in its ^1H NMR spectrum, consistent with the solid-state structure of **1** for two *cis* hydride ligands. In addition to the resonance of **1-d₁**, the hydride resonance for **1** was also present in the ^1H NMR spectrum, which showed isotope shift effects.²² The reported phosphinito-bridged Pt(I) complex $[(\text{PHCY}_2)\text{Pt}(\mu\text{-PCY}_2)\{k^2P,O\text{-}P(O)\text{CY}_2\}\text{Pt}(\text{PHCY}_2)](\text{Pt}\text{-Pt})$ was also found to activate hydrogen reversibly in solution under mild conditions, where the dihydride complex was shown to form through the nonclassical dihydrogen intermediate.⁵³

In solution, complex **2** catalyzes $\text{H}_2\text{-D}_2$ exchange to produce HD at room temperature as detected by ^1H NMR:

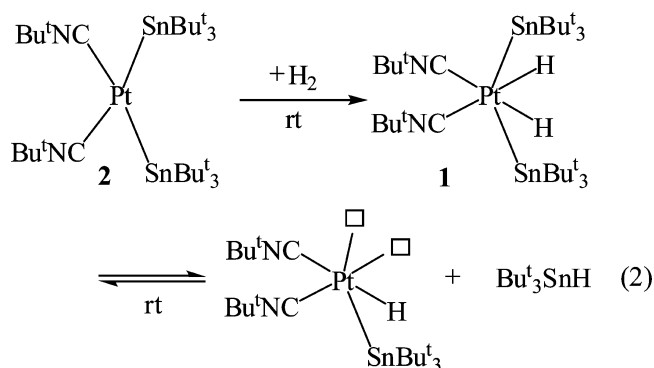


Integration of the peaks in the ^1H NMR spectrum yields $K_{\text{eq}} \approx 3.6$, in keeping with the literature value.⁵⁴ The fact that **2** catalyzes $\text{H}_2\text{-D}_2$ exchange, and that its reaction with HD gas afforded a mixture of isotopomers of **1**, prompted additional investigation of potential reaction mechanisms for the exchange process. Since addition of H_2 to **2** produces **1**, an 18-electron complex with no vacant site for additional

Scheme 1



binding, reductive elimination of stannane was considered, as shown in eq 2:



In the mechanism shown in eq 2, the active catalyst for H_2 - D_2 exchange would involve as a first step not elimination of H_2 from 1 to regenerate 2 but reductive elimination of Bu^t_3SnH to produce the intermediate complex $Pt(SnBu^t_3)(CNBu^t_3)_2(H)$, which would be the true catalyst for H_2 - D_2 exchange. To further probe this, we performed the reaction of the dideutride complex $Pt(SnBu^t_3)_2(CNBu^t_3)_2(D)_2$, **1-d₂**, and free Bu^t_3SnH . When an equimolar mixture of **1-d₂** and Bu^t_3SnH was placed in an NMR tube, $^2H\{^1H\}$ NMR revealed formation of Bu^t_3SnD , showing appropriate one-bond coupling to both ^{119}Sn and ^{117}Sn ($\delta = 5.62$, $^1J_{^{119}Sn-D} = 213$ Hz and $^1J_{^{117}Sn-D} = 203$ Hz). The deuteride region showed a peak at $\delta = -13.48$ ($^1J_{Pt-H} = 106$ Hz) due to **1-d₂** and **1-d₁**, and appropriately 1H NMR showed a resonance at $\delta = -13.49$ for **1-d₁** and -13.52 for **1**. These exchange experiments further support the proposed eq 2 for the H_2 - D_2 exchange mechanism to form HD gas. Based upon these experimental findings, Scheme 1 may be proposed for the catalytic formation of HD gas from H_2 - D_2 in the presence of compound 2.

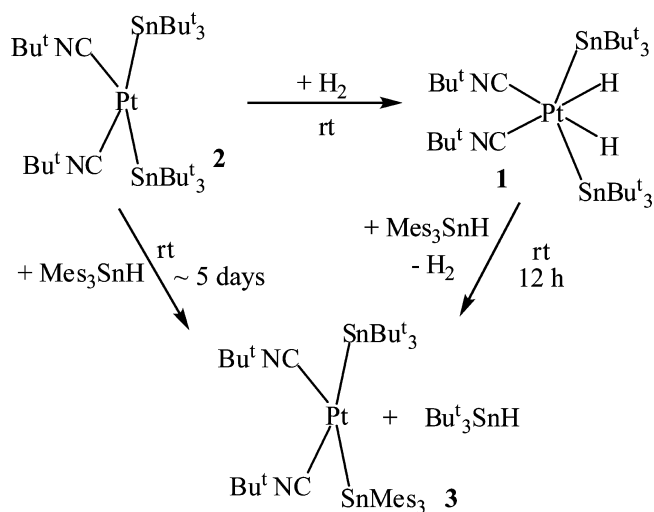
The catalytic cycle begins with the formation of **1**, followed by the reductive elimination of Bu^t_3SnH to form intermediate **A** with two vacant coordination sites. Step I is believed to be the rate-determining step. H_2/D_2 can then oxidatively add to the intermediate **A** to form another intermediate **B**. HD gas can then form by exchange of the H and D groups to

regenerate **A**. Steps II and III are repeated until equilibrium is reached. Once the catalytic cycle is completed, free Bu^t_3SnH formed during step I can add to intermediate **A** (step IV) to give back compound **1**.

In order to further probe a mechanism in which the proposed intermediate complex $Pt(SnBu^t_3)(CNBu^t_3)_2(H)$ was the active species, it was decided to see if substrates other than H_2 could be added. To test this we investigated the relative rates of reaction of Mes_3SnH and **2** in the presence and absence of H_2 . In the absence of added H_2 , production of the mixed stannane complex $Pt(SnMes_3)(SnBu^t_3)(CNBu^t_3)_2$, **3**, from $Pt(SnBu^t_3)_2(CNBu^t_3)_2$ and Mes_3SnH required more than 5 days to complete. Surprisingly, addition of H_2 to **2**, generating **1**, led to a more rapid production of **3**. These observations are in keeping with the mechanism shown in Scheme 2.

Direct conversion of **2** to **3** would necessarily involve oxidative addition of Mes_3SnH to **2** as a first step, but steric factors presumably do not favor this pathway. In the presence of H_2 , conversion of **2** to **1** could allow more facile stannane

Scheme 2



exchange by a mechanism similar to that proposed for H₂-D₂ exchange in Scheme 1—namely reductive elimination of Bu^t₃SnH to generate Pt(SnBu^t₃)(CNBu^t)₂(H), which could then undergo oxidative addition of Mes₃SnH, followed by reductive elimination of H₂, to yield the mixed stannane complex **3**. A variety of exchange reactions at the Pt metal center are reported in the literature,^{55–59} but to the authors' knowledge this is the first example of this type of stannane exchange reaction. It proved possible to isolate and structurally characterize the mixed stannane complex **3**, which is shown in Figure 3.

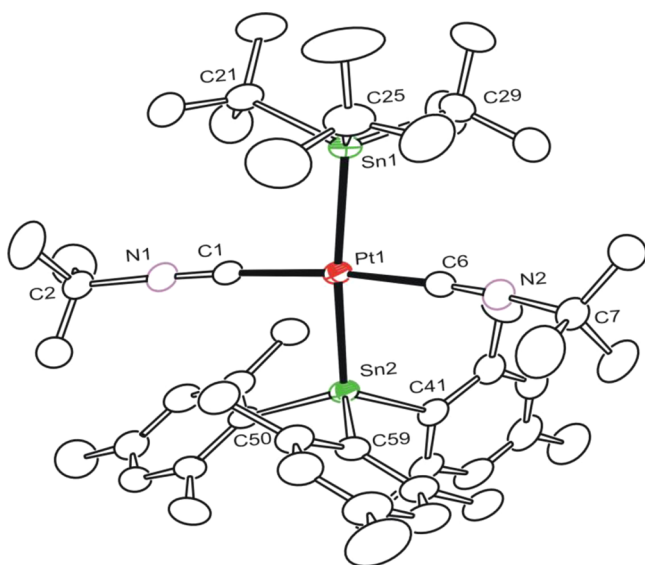


Figure 3. ORTEP⁵² drawing of the molecular structure of Pt(SnMes₃)(SnBu^t₃)(CNBu^t)₂, **3**, showing 30% probability thermal ellipsoids. Selected interatomic distances (Å) and angles (deg): Sn(1)–Pt(1) = 2.6797(5); Sn(2)–Pt(1) = 2.6775(5); C(1)–Pt(1) = 1.947(6); C(6)–Pt(1) = 1.945(6); Sn(1)–Pt(1)–Sn(2) = 171.50(2); C(1)–Pt(1)–C(6) = 167.1(3); C(6)–Pt(1)–Sn(1) = 92.1(2); C(1)–Pt(1)–Sn(1) = 93.3(2); C(1)–Pt(1)–Sn(2) = 89.3(2); C(6)–Pt(1)–Sn(2) = 87.0(2).

Compound **3** is similar in structure to **2**, where in place of one of the SnBu^t₃ there is an SnMes₃ group. The complex is not square planar, but at the same time it is not as distorted to a “saw-horse”-type structure as in **2** [C(1)–Pt(1)–C(6) = 167.1(3)°; Sn(1)–Pt(1)–Sn(2) = 171.50(2)°]. Complex **3** does not contain any hydride ligands, but it can be assumed that the dihydride complex Pt(SnMes₃)(SnBu^t₃)(CNBu^t)₂(H)₂, **4**, forms first and in turn loses H₂ to give **3**. Considering how labile the hydride ligands are in **1**, it is not surprising that **4** could not be detected. Furthermore, addition of H₂ to **3** does not occur, as in the case with **2** at room temperature.

Efforts to exchange the other SnBu^t₃ ligand from compound Pt(SnMes₃)(SnBu^t₃)(CNBu^t)₂, **3**, with an excess of Mes₃SnH to form the compound Pt(SnMes₃)₂(CNBu^t)₂, **5**, were unsuccessful at room temperature. However, we were able to prepare **5** directly from the reaction of Pt(COD)₂ with 2 equiv of CNBu^t and Mes₃SnH at –78 °C in 80% yield. A crystal structure of **5** is shown in Figure 4. Compound **5** is similar in structure to compound **3**, and it is also unreactive toward H₂ at room temperature, as in the case of **3**.

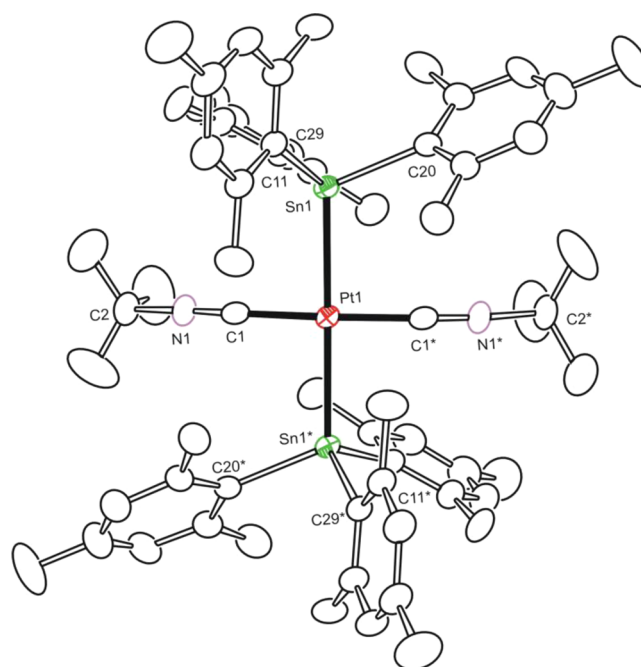


Figure 4. ORTEP⁵² drawing of the molecular structure of Pt(SnMes₃)₂(CNBu^t)₂, **5**, showing 30% probability thermal ellipsoids. Selected interatomic distances (Å) and angles (deg): Sn(1)–Pt(1) = 2.6615(6); C(1)–Pt(1) = 1.92(1); Sn(1)–Pt(1)–Sn(1*) = 175.74(3); Sn(1)–Pt(1)–C(1) = 89.0(3); C(1)–Pt(1)–C(1*) = 164.2(4).

Reaction of complex **2** with 3 equiv of Ph₃SnH (which is not as bulky as Bu^t₃SnH) at room temperature resulted in formation of the colorless tri-tin–platinum compound Pt(SnPh₃)₃(CNBu^t)₂(H), **6**, which was characterized by a combination of IR, ¹H NMR, elemental, and single-crystal X-ray diffraction analyses. In complex **6**, the two Bu^t₃Sn ligands in **2** have reacted with 2 equiv of Ph₃SnH, resulting in stannane exchange, and a third mole of Ph₃SnH has undergone oxidative addition, yielding the 18-electron Pt(IV) complex in an octahedral geometry, as shown in Figure 5.

The crystal structure of complex **6** provides evidence of the steric crowding present when three stannyls are coordinated to Pt in addition to the two bulky isonitrile ligands. It seems unlikely that complex **6** would be stable if, rather than SnPh₃, the coordinating stannyls included the much bulkier SnBu^t₃. As pointed out above, this would be the case if stannyl exchange were to occur in the absence of added H₂.

The ¹H NMR of Pt(SnPh₃)₃(CNBu^t)₂(H), **6**, displayed temperature-dependent dynamics in solution, see Figure 6. The spectrum showed two broad resonances in the hydride region at 25 °C (δ = –6.42 and –11.91). As the temperature was decreased to –20 °C, two distinct hydride resonances were observed, showing coupling to both platinum and tin (δ = –6.62, ¹J_{Sn–H} = 679 Hz, ¹J_{Pt–H} = 647 Hz, ¹J_{Pt–H} = 775 Hz, and δ = –11.90, ¹J_{Pt–H} = 665 Hz, ²J_{Sn–H} = 26.68 Hz, ²J_{Pt–H} = 13.95 Hz).

This is consistent with the presence of isomers in solution. Both hydride resonances show one-bond coupling to platinum. The resonance at –6.62 ppm also shows large coupling to tin. A plausible explanation of the NMR spectroscopic data is the equilibrium shown in Scheme 3. The large value of ¹J_{Sn–H} observed by us suggests the hydride ligand is *trans* to a SnPh₃, in keeping with literature

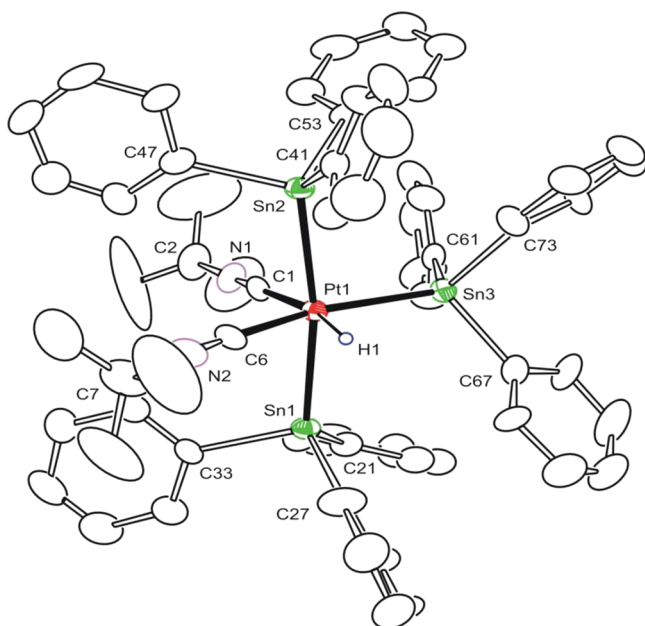


Figure 5. ORTEP⁵² drawing of the molecular structure of $\text{Pt}(\text{SnPh}_3)_3(\text{CNBU}^t)_2(\text{H})$, **6**, showing 30% probability thermal ellipsoids. Selected interatomic distances (Å) and angles (deg): $\text{Pt}(1)-\text{Sn}(1) = 2.6761(8)$; $\text{Pt}(1)-\text{Sn}(3) = 2.6140(7)$; $\text{Pt}(1)-\text{C}(1) = 2.03(1)$; $\text{Pt}(1)-\text{H}(1) = 1.65(6)$; $\text{Sn}(1)-\text{Pt}(1)-\text{Sn}(2) = 171.07(3)$; $\text{Sn}(2)-\text{Pt}(1)-\text{Sn}(3) = 93.32(2)$; $\text{C}(1)-\text{Pt}(1)-\text{Sn}(3) = 94.1(3)$; $\text{C}(1)-\text{Pt}(1)-\text{C}(6) = 102.8(4)$; $\text{Sn}(2)-\text{Pt}(1)-\text{C}(1) = 89.2(3)$; $\text{Sn}(1)-\text{Pt}(1)-\text{C}(6) = 85.0(3)$; $\text{C}(6)-\text{Pt}(1)-\text{H}(1) = 66(2)$; $\text{Sn}(3)-\text{Pt}(1)-\text{H}(1) = 97(2)$.

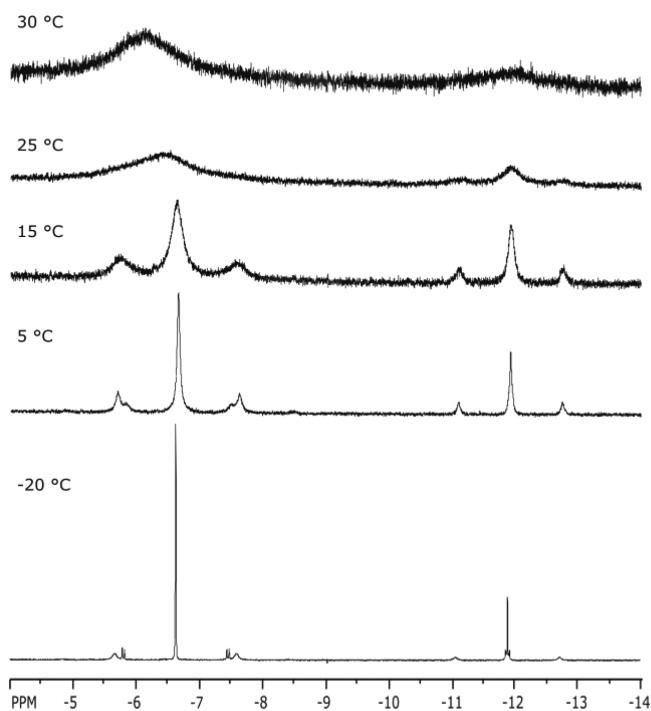


Figure 6. ^1H NMR spectra of $\text{Pt}(\text{SnPh}_3)_3(\text{CNBU}^t)_2(\text{H})$, **6**, at various temperatures.

data for related systems.^{60–63} In the previously reported octahedral iridium complex $[\text{Et}_3\text{NMe}]_2[\text{IrH}(\text{SnB}_{11}\text{H}_{11})_2(\text{CO})(\text{PPh}_3)_2]$, the hydride and both tin ligands are meridional and lie in the same plane along with the CO group, such that the

hydride is both *cis* and *trans* to the $\text{SnB}_{11}\text{H}_{11}$ ligands. The value for *trans*-two-bond coupling in this compound was reported to be 632 Hz, which is similar to the value we obtained.⁶⁰ In addition, *trans*-two-bond coupling in other Ir octahedral complexes has also been reported to be similar as well as larger and comparable to the one-bond coupling in Ph_3SnH .^{61–63}

This results in the possibility of two additional isomers for the SnPh_3 groups. The isomer **6A** retains *meridional* arrangement of the SnPh_3 but has the CNBU^t groups in the *trans* position. Isomer **6B** is viewed as unlikely since it places the three SnPh_3 groups in a *facial* arrangement. We have tried several times, at low temperatures as well, to identify the structure of the isomer in solution by single-crystal X-ray diffraction but were only able to obtain crystals of the *cis* hydride complex **6**. As the temperature is raised from -20 °C, the two hydride signals start to broaden and coalesce; however, the averaged fast exchange limit could not be obtained, as the complex decomposes above 30 °C.

Compound $\text{Pt}(\text{SnPh}_3)_3(\text{CNBU}^t)_2(\text{H})$, **6**, is unstable in air, loses hydride and Ph_3Sn ligands as H_2 and $\text{Ph}_3\text{Sn}-\text{SnPh}_3$, and forms a stable yellow colored compound, $\text{Pt}(\text{SnPh}_3)_2(\text{CNBU}^t)_2$, **7**. Compound **7** can also be prepared by reacting $\text{Pt}(\text{COD})_2$ with 2 equiv each of Ph_3SnH and CNBU^t at -78 °C and allowing it to warm to room temperature. The complex was characterized by a combination of IR, ^1H NMR, elemental, and single-crystal X-ray diffraction analyses. An ORTEP drawing of the molecular structure of **7** is shown in Figure 7.

It is of interest that compound **7** reacts with Ph_3SnH under argon to give back compound **6**, but it does not react with H_2 to produce $\text{Pt}(\text{SnPh}_3)_2(\text{CNBU}^t)_2(\text{H})_2$. In keeping with this is the fact that compound **7** can be produced directly by reaction of 2 mol of Ph_3SnH with $\text{Pt}(\text{COD})_2$ in the presence of CNBU^t at -78 °C, followed by warming to room temperature. The reaction corresponding to production of the dihydride **1** does not yield the corresponding dihydride $\text{Pt}(\text{SnPh}_3)_2(\text{CNBU}^t)_2(\text{H})_2$ which if formed must reductively eliminate H_2 to yield **7**. The observed failure of $\text{Pt}(\text{SnPh}_3)_2(\text{CNBU}^t)_2$ to add H_2 is therefore ascribed to thermodynamic rather than kinetic factors. While **7** does not react with H_2 it does react readily with Ph_3SnH undergoing oxidative addition to form **6**. This is presumably due to the greater H–H bond strength (104 kcal/mol) compared to the H– SnPh_3 bond strength (~ 74 kcal/mol)^{64,65} tempered by the corresponding bond strengths to Pt since steric factors would overwhelmingly favor H_2 addition.

Both the trimesityltin and triphenyltin analogues **5** and **7** do not add H_2 , nor do they catalyze H_2 – D_2 exchange. This could be due to steric factors, but electronic influence could conceivably play a role since these two complexes contain aryl groups pendant on tin versus the electronically different to alkyl tri-*tert*-butyl groups of **2**. In order to test this, the triisopropyl analogue $\text{Pt}(\text{SnPr}^i)_2(\text{CNBU}^t)_2$, **8**, was prepared by the reaction of $\text{Pt}(\text{COD})_2$ with 2 equiv each of Pr^i_3SnH and CNBU^t . The crystal structure of **8** is shown in Figure 8, and it is nearly square planar, with the angles about platinum just shy of 180° , at 177° for $\text{Sn}1^*-\text{Pt}1-\text{Sn}1$ and 176° for $\text{C}1-\text{Pt}1-\text{C}2$. Since the electronic donor properties of the trialkyltin ligands in **8** should closely resemble those in **2**, the observed structural difference is attributed to steric rather than electronic factors.

Scheme 3

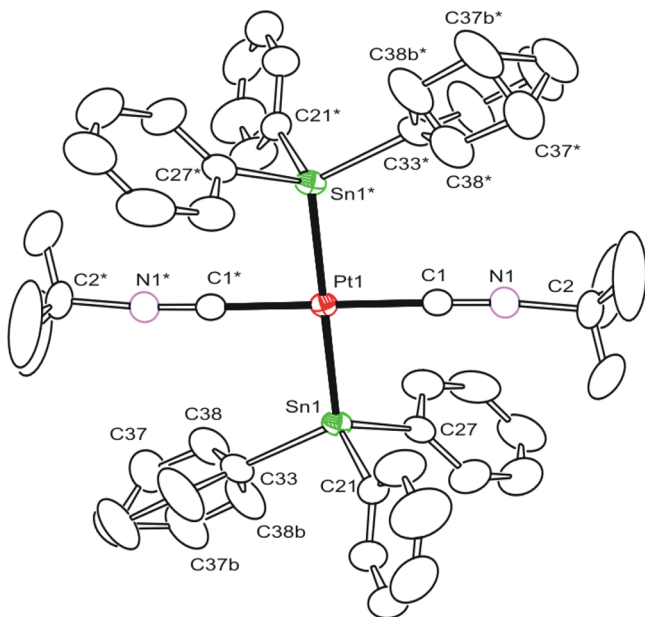
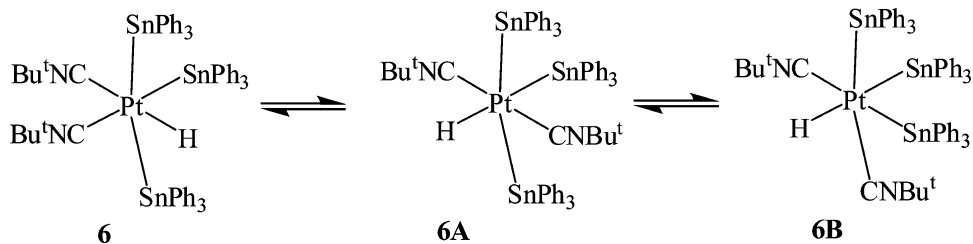


Figure 7. ORTEP⁵² drawing of the molecular structure of $\text{Pt}(\text{SnPh}_3)_2(\text{CNBu}^t)_2$, **7**, showing 30% probability thermal ellipsoids. One of the Ph groups on Sn is disordered, as shown in C37 and C38. Selected interatomic distances (Å) and angles (deg): Pt(1)–Sn(1) = 2.6231(3); Pt(1)–C(1) = 1.936(5); Sn(1)–Pt(1)–Sn(1*) = 180.00; Sn(1)–Pt(1)–C(1) = 87.5(1); Sn(1)–Pt(1)–C(1*) = 92.5(1); C(1)–Pt(1)–C(1*) = 180.0(2).

The consequences of these steric differences are displayed in differing reactivity patterns as well. Complex **8** does not add H_2 at room temperature to give $\text{Pt}(\text{SnPr}^i)_2(\text{CNBu}^t)_2(\text{H})_2$, nor does it catalyze H_2 – D_2 exchange. Qualitative understanding of the forces involved in determining whether oxidative addition occurs or not is aided by looking at the starting structures shown in Figure 9 for the four complexes $\text{Pt}(\text{SnR}_3)_2(\text{CNBu}^t)_2$ ($\text{R} = \text{Bu}^t, \text{Mes}, \text{Ph}, \text{or Pr}^i$).

Based on the large number of square planar d^8 complexes of Pt(II), it is clear that this is the preferred and lowest energy geometry in the absence of complicating steric or electronic effects. The complexes $\text{Pt}(\text{SnPh}_3)_2(\text{CNBu}^t)_2$, **7**, and $\text{Pt}(\text{SnPr}^i)_2(\text{CNBu}^t)_2$, **8**, closely approximate this geometry, but $\text{Pt}(\text{SnMes}_3)_2(\text{CNBu}^t)_2$, **5**, and particularly $\text{Pt}(\text{SnBu}^t)_2(\text{CNBu}^t)_2$, **2**, deviate from it substantially. The fact that H_2 addition occurs only in the sterically most crowded system is counter-intuitive and must be due to electronic effects placing it at a higher starting energy. This is illustrated in eq 3 for the oxidative addition of H_2 :

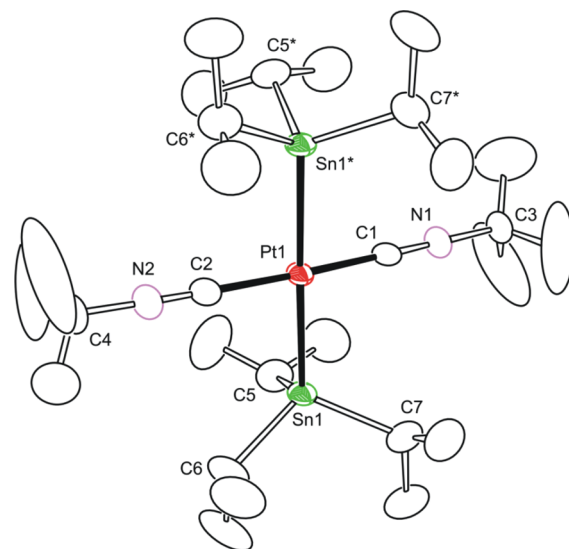


Figure 8. ORTEP⁵² drawing of the molecular structure of $\text{Pt}(\text{SnPr}^i)_2(\text{CNBu}^t)_2$, **8**, showing 30% probability thermal ellipsoids. Selected interatomic distances (Å) and angles (deg): Pt(1)–Sn(1) = 2.6390; Pt(1)–C(1) = 1.901; Pt(1)–C(2) = 1.929; Sn(1)–Pt(1)–Sn(1*) = 177.18; C(1)–Pt(1)–C(2) = 175.8; C(1)–Pt(1)–Sn(1) = 88.9; C(2)–Pt(1)–Sn(1) = 91.0.

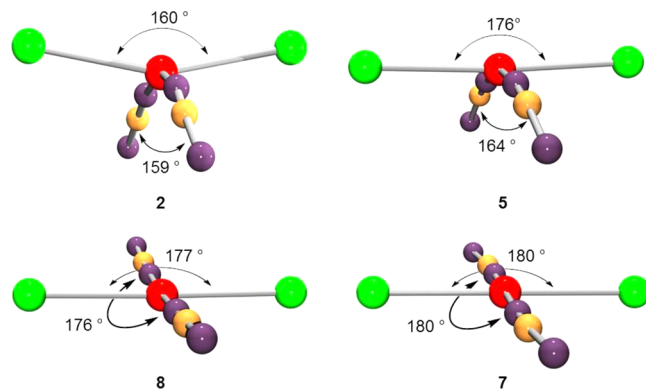
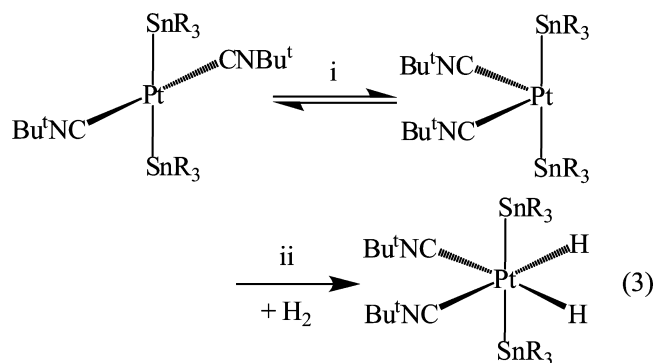


Figure 9. Comparison of the structures of **2**, **5**, **7**, and **8** (R groups omitted for clarity). Colors: Pt, red; Sn, green; C, purple; N, gold. Shown are the Sn–Pt–Sn and C–Pt–C (C atom bonded to Pt) angles.



The net thermochemistry of oxidative addition of H_2 to square planar Pt(II) complex can be envisioned as a two-step process, as shown in eq 3. The first step involves rearrangement to a “saw-horse”-type structure, followed by a second step in which H_2 addition occurs. Since the square planar geometry is preferred, this step is expected to be endothermic and to be compensated for in the second step, which is exothermic addition of H_2 to a complex already exhibiting an optimal final ligand geometry. This logic applies to the complexes **5**, **7**, and **8**, which have a ground state that is “essentially” square planar. The fact that H_2 addition does not occur to produce equilibrium amounts of dihydride is attributed to the fact that the isomerization energy is not fully compensated for by the oxidative addition of dihydrogen. In the case of complex **2**, which is ground state destabilized due to the steric bulk of its ligand set, this price does not have to be paid, since the core final geometry of the H_2 oxidative addition product closely resembles that of the starting complex **2**. This effect is expected to apply to both the enthalpy and entropy of oxidative addition of dihydrogen, and detailed thermochemical studies of this effect are in progress.

The hydride ligands in **1** are labile and eliminate under mild conditions. We were fortunate to isolate complex **1** in pure form and obtain its crystal structure. In keeping with the arguments above, we were unable to isolate the analogous carbonyl complex $Pt(SnBu^t_3)_2(CO)_2(H)_2$ when the reaction of $Pt(COD)_2$ with Bu^t_3SnH was carried out at room temperature under an atmosphere of carbon monoxide gas. Instead, we were only able to isolate the carbonyl complex $Pt(SnBu^t_3)_2(CO)_2$, **9**, in 91% yield, which does not contain any hydride ligands. The structure of **9** is shown in Figure 10, and as expected for platinum(II) complexes in a d^8 configuration, the molecular geometry is square planar. It is interesting to note that the ligands are *trans* and that the structure of **9** is planar rather than deviating considerably from planarity as in **2**, which can be accounted for by the sterics of the $CNBu^t$ ligands versus the CO ligands as seen in Figure 10. A similar Pt–Ge complex, *trans*- $Pt(CO)_2(GePh_3)_2$, which was obtained from the reaction of $Pt(COD)Me_2$ and $HGePh_3$ in the presence of CO atmosphere, has Pt–C(CO) bond lengths and Ge–Pt–C(CO) bond angles similar to those of compound **9**.⁶⁶ Most relevant to this work is the fact that complex **9** does not add H_2 , supporting the idea that perturbation of the stable square planar structure, exhibited for **2** but not for **9**, plays a key role in oxidative addition.

The carbonyl ligands in **9** can be replaced with $CNBu^t$ groups to give compound **2**; however, en route to **2**, we obtained the complex $Pt(SnBu^t_3)_2(CNBu^t)_2(CO)$, **10**, in 96% yield at room temperature. The structure of **10** is given in Figure 11. The molecular geometry of complex **10** is trigonal

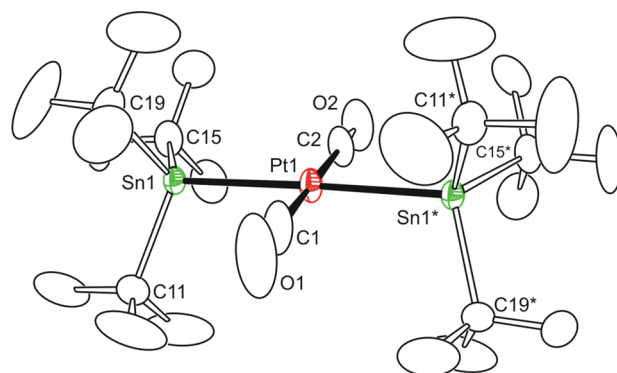


Figure 10. ORTEP⁵² drawing of the molecular structure of $Pt(SnBu^t_3)_2(CO)_2$, **9**, showing 30% probability thermal ellipsoids. Selected interatomic distances (Å) and angles (deg): Pt(1)–Sn(1) = 2.7317(4); Pt(1)–Sn(1*) = 2.7317(4); Pt(1)–C(1) = 1.847(1); Pt(1)–C(2) = 1.894(1); Sn(1)–Pt(1)–Sn(1*) = 176.08(2); C(1)–Pt(1)–C(2) = 180.0(6); Sn(1)–Pt(1)–C(1) = 88.0(5); Sn(1)–Pt(1)–C(2) = 92.0(4).

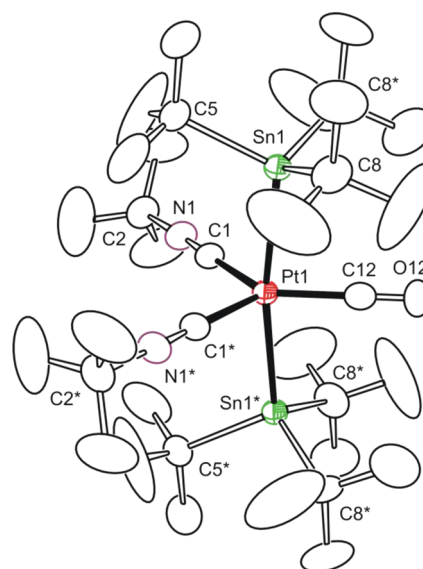
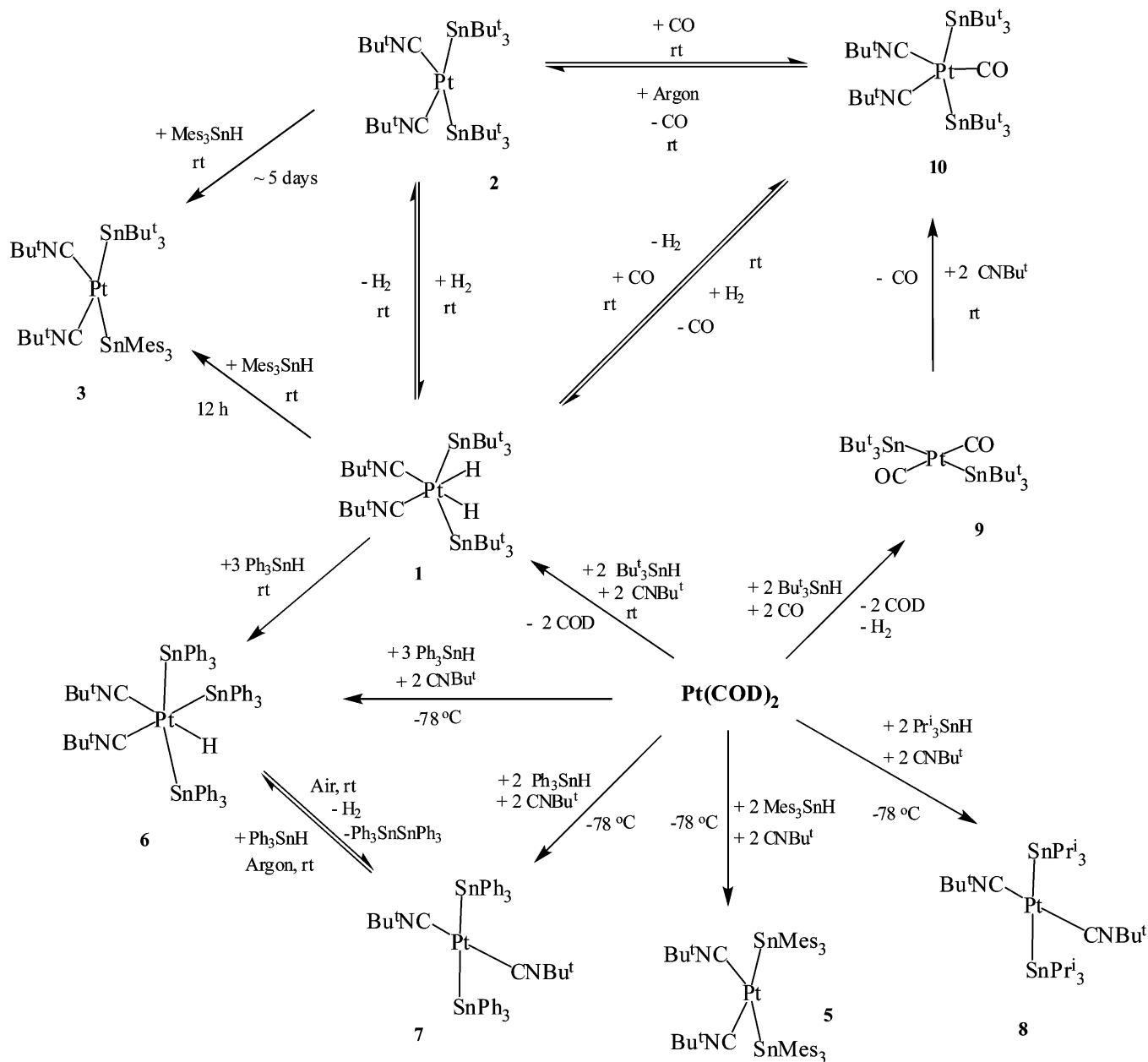


Figure 11. ORTEP⁵² drawing of the molecular structure of $Pt(SnBu^t_3)_2(CNBu^t)_2(CO)$, **10**, showing 30% probability thermal ellipsoids. Selected interatomic distances (Å) and angles (deg): Pt(1)–Sn(1) = 2.7147(6); Pt(1)–C(1) = 2.02(1); Pt(1)–C(12) = 1.89(2); Sn(1)–Pt(1)–Sn(1*) = 170.66(3); C(1)–Pt(1)–C(12) = 128.2(6); Sn(1)–Pt(1)–C(1) = 92.9(3); Sn(1)–Pt(1)–C(12) = 85.3(5); C(1)–Pt(1)–C(1*) = 103.7(4).

bipyramidal, in which the two $SnBu^t_3$ groups occupy both of the axial positions, while the two $CNBu^t$ and one CO ligand lie in the equatorial plane. In solution, **10** can be readily converted to **2** at room temperature in 91% yield under a stream of argon gas. In the solid state as well (~16 h), **10** is converted to **2** in quantitative yields under a flow of argon gas. Although the number of steps is more to obtain **1** from **9**, rather than directly as described above, this pathway is “cleaner” and makes it easier to obtain **2** in pure form, which can then be converted to **1** as well.

There are very few examples of transition metal complexes with group 14 metals in a trigonal bipyramidal geometry, as in compound **10**, reported in the literature.^{47,67} The Ni–Sn compound, $Ni(SnBu^t_3)_2(CO)_3$, previously reported by us, is structurally close to **10**. The CO ligands on the Ni metal

Scheme 4



center in this complex are not labile as in the case of compound **10**.⁴⁷

SUMMARY AND CONCLUSIONS

Scheme 4 presents a summary for the synthesis of various Pt-Sn hetero-bimetallic complexes. A series of Pt(II)-Sn bimetallic complexes of the type $\text{Pt}(\text{SnR}_3)_2(\text{CNBu}^t)_2$ ($\text{R} = \text{Bu}^t, \text{Mes}, \text{Ph}, \text{Pr}^i$) were prepared and studied. The Pt(IV) dihydride compound **1** reversibly loses both hydrides to furnish Pt(II) compound **2**. Compound **2** is not square planar, and the observed geometry resembles a “saw-horse” structure due to the sterics of bulky Bu^t groups. Compounds **2** and **1** are inter-convertible even in the solid state. Compound **2** activates hydrogen reversibly even at -78°C , with no observable decrease in the rate of the reaction. It also catalyzes H_2 - D_2 exchange to form HD gas, and the proposed mechanism involves the reductive elimination of Bu^t_3SnH to

create vacant coordination sites on the platinum metal center to facilitate H_2 - D_2 exchange. The rate of exchange was found to be independent of Bu^t_3SnH . The SnBu^t_3 group from **1** can be replaced with Mes_3SnH to give Pt(II) compound **3** with two different tin ligands on the same platinum metal center. The SnBu^t_3 groups from **1** can also be replaced with Ph_3Sn to give the sterically strained Pt(IV) compound **6** with three terminal tin ligands on the same platinum metal center. Compound **6** displays fluxional behavior in the solution, with plausible *cis-trans* isomerization. It decomposes in air to form Pt(II) compound **7**. Though compound **7** is sterically not too crowded, this square planar compound is also stable to H_2 addition, but interestingly it reacts with Ph_3SnH to regenerate the octahedral compound **6**. The triisopropyltin analogue $\text{Pt}(\text{SnPr}^i_3)_2(\text{CNBu}^t)_2$, **8**, also does not catalyze H_2 - D_2 exchange. The reaction of $\text{Pt}(\text{COD})_2$ with Bu^t_3SnH and carbon monoxide gas yielded square planar Pt(II) compound

9, with CO ligands *trans* to each other. Compound 9 is also unreactive toward H₂, but it loses a CO ligand in the presence of CNBu^t to give the trigonal bipyramidal compound 10, which subsequently can lose another CO ligand to furnish 2 or 1.

The fact that in this series of complexes it is only 2 that reversibly adds H₂ and participates in catalytic H₂–D₂ exchange is attributed to the fact that in this bulky complex a “steric threshold” has been crossed.⁶⁸ Due to steric factors attributed to the bulky ancillary SnBu₃ ligands, complex 2 is forced away from the more stable square planar geometry to a “saw-horse” structure; the Sn–Pt–Sn angle (159.5°) in 2 closely resembles that of its dihydride adduct 1 (161.3°), resulting in a more favorable reaction profile. The role of pendant groups on trialkylphosphine ligands in controlling oxidative addition of dihydrogen has been intensively investigated since the pioneering work of Kubas and others.^{70,71} This work demonstrates that the pendant groups in trialkyltin and triaryltin complexes can also fine-tune reactivity with respect to H₂ addition and H₂–D₂ exchange.

■ ASSOCIATED CONTENT

■ Supporting Information

CIF files and details for each of the structural analyses. This material is available free of charge via the Internet at <http://pubs.acs.org>.

■ AUTHOR INFORMATION

Corresponding Author

captain@miami.edu

Notes

The authors declare no competing financial interest.

■ ACKNOWLEDGMENTS

The National Science Foundation (CHE-1300206) is gratefully acknowledged for support of this work as well as for providing funds toward the purchase of a LC-ESI-MS (CHE-0946858).

■ REFERENCES

- (1) Donaldson, J. D. *Prog. Inorg. Chem.* **1968**, *8*, 287–356.
- (2) Brooks, E. H.; Cross, R. J. *Organomet. Chem. Rev.* **1970**, *6A*, 227.
- (3) Holt, M. S.; Wilson, W. L.; Nelson, J. H. *Chem. Rev.* **1989**, *89*, 11–49.
- (4) Cramer, R. D.; Jenner, E. L.; Lindsey, R. V.; Stolberg, U. G. *J. Am. Chem. Soc.* **1963**, *85*, 1691–1692.
- (5) Parshall, G. W. *J. Am. Chem. Soc.* **1966**, *88*, 704–708.
- (6) Schwager, I.; Knifton, J. F. *J. Catal.* **1976**, *45*, 256–267.
- (7) Tsuji, Y.; Shida, J.; Takeuchi, R.; Watanabe, Y. *Chem. Lett.* **1984**, 889–890.
- (8) Coupé, J. N.; Jordão, E.; Fraga, M. A.; Mendes, M. J. *Appl. Catal. A: Gen.* **2000**, *199*, 45–51.
- (9) Muraza, O.; Rebrov, E. V.; Berenguer-Murcia, A.; de Croon, M. H. J. M. *Appl. Catal. A: Gen.* **2009**, *368*, 87–96.
- (10) Zhu, L.; Yempally, V.; Isrow, D.; Pellechia, P. J.; Captain, B. J. *Organomet. Chem.* **2010**, *695*, 1–5.
- (11) Hungria, A. B.; Raja, R.; Adams, R. D.; Captain, B.; Thomas, J. M.; Midgley, P. A.; Golovko, V.; Johnson, B. F. G. *Angew. Chem., Int. Ed.* **2006**, *45*, 4782–4785.
- (12) Adams, R. D.; Boswell, E. M.; Captain, B.; Hungria, A. B.; Midgley, P. A.; Raja, R.; Thomas, J. M. *Angew. Chem., Int. Ed.* **2007**, *46*, 8182–8185.
- (13) Adams, R. D.; Trufan, E. *Philos. Trans. R. Soc. A* **2010**, *368*, 1473–1493.
- (14) Kuwabara, T.; Guo, J. D.; Nagase, S.; Saito, M. *Angew. Chem., Int. Ed.* **2014**, *53*, 434–438.
- (15) West, J. K.; Fondong, G. L.; Noll, B. C.; Stahl, L. *Daltan Trans.* **2013**, *42*, 3835–3842.
- (16) Wagner, M.; Deáky, V.; Dietz, C.; Martincová, J.; Mahieu, B.; Jambor, R.; Herres-Pawlis, S.; Jurkschat, K. *Chem.—Eur. J.* **2013**, *19*, 6695–6708.
- (17) Cabeza, J. A.; Fernández-Colinas, J. M.; García-Álvarez, P.; Polo, D. *Inorg. Chem.* **2012**, *51*, 3896–3903.
- (18) Henning, J.; Wesemann, L. *Angew. Chem., Int. Ed.* **2012**, *51*, 12869–12873.
- (19) Al-Rafia, S. M. I.; Malcolm, A. C.; Liew, S. K.; Ferguson, M. J.; McDonald, R.; Rivard, E. *Chem. Commun.* **2011**, *47*, 6987–6989.
- (20) Martincová, J.; Dostál, L.; Herres-Pawlis, S.; Růžička, A.; Jambor, R. *Chem.—Eur. J.* **2011**, *17*, 7423–7427.
- (21) Hornung, M.; Wesemann, L. *Eur. J. Inorg. Chem.* **2010**, 2949–2955.
- (22) Yempally, V.; Zhu, L.; Captain, B. *Inorg. Chem.* **2010**, *49*, 7238–7240.
- (23) Alvarez, M. A.; García, M. E.; García-Vivó, D.; Ruiz, M. A.; Vega, M. F. *Organometallics* **2010**, *29*, 512–515.
- (24) Adams, R. D.; Blom, D. A.; Captain, B.; Raja, R.; Thomas, J. M.; Trufan, E. *Langmuir* **2008**, *24*, 9223–9226.
- (25) Filippou, A. C.; Portius, P.; Philippopoulos, A. I.; Rohde, H. *Angew. Chem., Int. Ed.* **2003**, *42*, 445–447.
- (26) Eichler, B. E.; Phillips, A. D.; Haubrich, S. T.; Mork, B. V.; Power, P. P. *Organometallics* **2002**, *21*, 5622–5627.
- (27) Agustín, D.; Rima, G.; Gornitzka, H.; Barrau, J. *Eur. J. Inorg. Chem.* **2000**, *2000*, 693–702.
- (28) Sinfelt, J. H. *Bimetallic Catalysts. Discoveries, Concepts and Applications*; Wiley: New York, 1983.
- (29) Burch, R.; Garla, L. C. *J. Catal.* **1981**, *71*, 360–372.
- (30) Burch, R. *J. Catal.* **1981**, *71*, 348–359.
- (31) Srinivasan, R.; Davis, B. H. *Platin. Met. Rev.* **1992**, *36*, 151–163.
- (32) Fujikawa, T.; Ribeiro, F. H.; Somorjai, G. A. *J. Catal.* **1998**, *178*, 58–65.
- (33) Park, Y.-K.; Ribeiro, F. H.; Somorjai, G. A. *J. Catal.* **1998**, *178*, 66–75.
- (34) Thomas, J. M.; Johnson, B. F. G.; Raja, R.; Sankar, G.; Midgley, P. A. *Acc. Chem. Res.* **2003**, *36*, 20–30.
- (35) Hermans, S.; Raja, R.; Thomas, J. M.; Johnson, B. F. G.; Sankar, G.; Gleeson, D. *Angew. Chem., Int. Ed.* **2001**, *40*, 1211–1215.
- (36) Johnson, B. F. G.; Raynor, S. A.; Brown, D. B.; Shephard, D. S.; Mashmeyer, T.; Thomas, J. M.; Hermans, S.; Raja, R.; Sankar, G. *J. Mol. Catal. A: Chem.* **2002**, *182–183*, 89–97.
- (37) Hermans, S.; Johnson, B. F. G. *J. Chem. Soc., Chem. Commun.* **2000**, 1955–1956.
- (38) Huber, G. W.; Shabaker, J. W.; Dumesic, J. A. *Science* **2003**, *300*, 2075–2077.
- (39) Shabaker, J. W.; Simonetti, D. A.; Cortright, R. D.; Dumesic, J. A. *J. Catal.* **2005**, *231*, 67–76.
- (40) Jardine, I.; McQuillin, F. J. *Tetrahedron Lett.* **1966**, *7*, 4871–4875.
- (41) Bond, G. C.; Hellier, M. J. *J. Catal.* **1967**, *7*, 217–222.
- (42) D’Aniello, M. J.; Barefield, E. K. *J. Am. Chem. Soc.* **1978**, *100*, 1474–1481.
- (43) Watanabe, Y.; Tsuji, Y.; Suzuki, N. *Chem. Lett.* **1982**, *11*, 105–106.
- (44) Cheng, C.-H.; Eisenberg, R. *J. Am. Chem. Soc.* **1978**, *100*, 5968–5970.
- (45) Rocha, W. R. *J. Mol. Struct. (Theochem)* **2004**, *677*, 133–143.
- (46) Manzoli, M.; Shetti, V. N.; Blaine, J. A. L.; Zhu, L.; Isrow, D.; Yempally, V.; Captain, B.; Coluccia, S.; Raja, R.; Gianotti, E. *Daltan Trans.* **2012**, *41*, 982–989.
- (47) Yempally, V.; Zhu, L.; Isrow, D.; Captain, B. *J. Clust. Sci.* **2010**, *21*, 417–426.

- (48) Zhu, L.; Yempally, V.; Isrow, D.; Pellechia, P.; Captain, B. J. *Clust. Sci.* **2012**, *23*, 627–648.
- (49) Spencer, J. L. *Inorg. Synth.* **1979**, *19*, 213.
- (50) Gynane, M. J. S.; Lappert, M. F.; Riley, P. I.; Rivière, P.; Rivière-Baudet, M. J. *Organomet. Chem.* **1980**, *202*, 5–12.
- (51) Klingler, R. J.; Mochida, K.; Kochi, J. K. *J. Am. Chem. Soc.* **1979**, *101*, 6626–6637.
- (52) Farrugia, L. J. *J. Appl. Crystallogr.* **2012**, *45*, 849–854.
- (53) Mastrorilli, P.; Latronico, M.; Gallo, V.; Polini, F.; Re, N.; Marrone, A.; Gobetto, R.; Ellena, S. *J. Am. Chem. Soc.* **2010**, *132*, 4752–4765.
- (54) Urey, H. C. *J. Chem. Soc.* **1947**, 562–581.
- (55) Glockling, F.; Pollock, R. J. I. *J. Chem. Soc., Dalton Trans.* **1975**, 497–498.
- (56) Clemmit, A. F.; Glockling, F. *J. Chem. Soc., Chem. Commun.* **1970**, 705–706.
- (57) Tanabe, M.; Ito, D.; Osakada, K. *Organometallics* **2007**, *26*, 459–462.
- (58) Corey, J. Y. *Adv. Organomet. Chem.* **2004**, *51*, 1–52.
- (59) Curtis, M. D.; Epstein, P. S. *Adv. Organomet. Chem.* **1981**, *19*, 213–255.
- (60) Kirchmann, M.; Fleischhauer, S.; Wesemann, L. *Organometallics* **2008**, *27*, 2803–2808.
- (61) Kretschmer, M.; Pregosin, P. S.; Albinati, A.; Togni, A. *J. Organomet. Chem.* **1985**, *281*, 365–378.
- (62) Permin, A.; Eisenberg, R. *Inorg. Chem.* **2002**, *41*, 2451–2458.
- (63) Garralda, M. A.; Hernández, R.; Ibarlucea, L.; Pinilla, E.; Torres, M. R. *Organometallics* **2003**, *22*, 3600–3603.
- (64) Burkey, T. J.; Majewski, M.; Griller, D. *J. Am. Chem. Soc.* **1986**, *108*, 2218–2221.
- (65) Laarhoven, L. J. J.; Mulder, P.; Wayner, D. M. *Acc. Chem. Res.* **1999**, *32*, 342–349.
- (66) Adams, R. D.; Trufan, E. *Inorg. Chem.* **2009**, *48*, 6124–6129.
- (67) Curnow, O. J.; Nicholson, B. K.; Severinsen, M. J. *J. Organomet. Chem.* **1990**, *388*, 379–390.
- (68) The concept of a “steric threshold” could be analyzed utilizing a scale developed by Houser to quantify the distortion from square planar toward tetrahedral geometry,⁶⁹ which ranges from 0 (square planar) to 1 (tetrahedral). Utilizing that scale, the distortions of the complexes in Figure 9 are as follow: **7** (0.00) < **8** (0.05) < **5** (0.14) < **2** (0.29). The distortion of complex **2** is significant, but insufficient data are available at this time to delineate the exact position of a “steric threshold” for hydrogen addition in this reaction.
- (69) Yang, L.; Powell, D. R.; Houser, R. P. *Dalton Trans.* **2007**, 955–964.
- (70) Kubas, G. J.; Ryan, R. R.; Swanson, B. I.; Vergamini, P. J.; Wasserman, H. J. *J. Am. Chem. Soc.* **1984**, *106*, 451–452.
- (71) Kubas, G. J. *Chem. Rev.* **2007**, *107*, 4152–4205.